



Research Article

JOURNAL OF APPLIED PHARMACEUTICAL RESEARCH | JOAPR

www.japtronline.com

ISSN: 2348 – 0335

HOT MELT EXTRUSION AIDED AMORPHOUS SOLID DISPERSIONS OF QUERCETIN AND RESVERATROL FOR SOLUBILITY ENHANCEMENT

Lakshmi Swapna Sai¹, Fatima S Dasankoppa^{1*}, Srinivas Mutalik², Muralidhar Pisay²

Article Information

Received: 31st October 2024

Revised: 5th January 2025

Accepted: 29th January 2025

Published: 28th February 2025

Keywords

Hot melt extrusion, Amorphous solid dispersion, Soluplus, Quercetin, Resveratrol, Kolliphor, Polyvinylpyrrolidone

ABSTRACT

Background: Conversion of poorly soluble drugs into amorphous solid dispersions using different carriers is a formulation approach to improve solubility. **Objective:** The study investigates hot melt extrusion as an approach for producing amorphous solid dispersions that contribute to solubility enhancement. **Methodology:** Solid dispersions were hot melt extruded using two model compounds – quercetin and resveratrol with different carriers. The resulting solid dispersions were analyzed for solubility enhancement and characterized by various techniques. **Results and Discussion:** The solubility of solid dispersions was evaluated, revealing a 36-fold increase in the solubility of quercetin from 0.023 mg/ml to 0.823 mg/ml and a 97-fold increase in the solubility of resveratrol from 0.053 mg/ml to 5.125 mg/ml with soluplus as a carrier. Various characterization studies indicated the conversion of crystalline forms of quercetin and resveratrol into their amorphous forms, which was confirmed by powder x-ray crystallographic and scanning electron microscopic studies. In addition, the particle size reduction of quercetin reduced from 1.53 μm to 0.48 μm and resveratrol of 10.26 μm particle size was reduced to 0.22 μm in solid dispersions with soluplus as the carrier with decreased polydispersity index. **Conclusion:** This research demonstrates hot melt extrusion as a practical approach for fabricating amorphous solid dispersions.

INTRODUCTION

Almost all the drugs (90% that are under development process and about 40% of marketed drugs) have the problem of poor solubility, leading to poor absorption and bioavailability, which in turn results in minimal or low therapeutic efficacy of the drug [1]. Another major challenge in developing a poorly soluble drug into a dosage form is its *in vivo* absorption, which depends on

the apparent solubility and dissolution rate of the drug in the gastrointestinal tract. This can be addressed using a formulation approach, such as creating an amorphous solid dispersion (ASD). The dissolution rate of the drug can be enhanced due to the higher kinetic solubility of ASD compared to its crystalline form [2]. Formation of amorphous solid dispersions involves mechanisms like supersaturation, where the drug is incorporated

¹Department of Pharmaceutics, KLE College of Pharmacy, Vidyanagar, Hubballi (A constituent unit of KLE Academy of Higher Education and Research, Belagavi), Karnataka, India - 580031

²Department of Pharmaceutics, Manipal College of Pharmaceutical Sciences, Manipal Academy of Higher Education, Manipal, Karnataka, India 576104

*For Correspondence: fsdasankop@gmail.com

©2025 The authors

This is an Open Access article distributed under the terms of the Creative Commons Attribution (CC BY NC), which permits unrestricted use, distribution, and reproduction in any medium, as long as the original authors and source are cited. No permission is required from the authors or the publishers. (<https://creativecommons.org/licenses/by-nc/4.0/>)

into a matrix of the polymer or the carrier at a concentration higher than the solubility of the drug. Size reduction is another mechanism where forced induction of the drug into the polymeric carrier results in reduced particle size, increasing the surface area and resulting in improved dissolution. Amorphous solid dispersions are highly soluble than those of crystalline forms of the drugs. Thus, amorphous solid dispersions can increase solubility, enhance bioavailability, or both in some instances [3].

Usually, ASDs formed by various methods are glassy and are less thermodynamically stable than the crystalline forms during storage. So, the manufacturing process employed in fabricating ASDs plays a key role in determining the dispersion properties [4]. Techniques like hot melt extrusion (HME) and spray drying are mostly used for industrial scale production of ASDs. Yet, hot melt extrusion is preferred over spray drying because of certain advantages like fabrication of ASDs without employing any solvents, better scalability, precise control of process parameters, ease of handling and improving batch size, etc., resulting in employing HME more than that of spray, drying techniques [5]. Various properties, such as the drug's tendency to crystallize, glass transition, molecular mobility, drug-polymer miscibility, etc., affect the stability of ASDs [6]. The characteristics of amorphous solid dispersions based on preparation technique may result in processing difficulties during the formulation of solid dispersions into a dosage form.

In the process of extrusion during HME, ASD was formed due to mechanical energy produced by rotating screws and barrel, resulting in thermal energy which exerts on the physical mixture and aids in the conversion of the blend into an amorphous solid dispersion [7]. The hot melt extrusion technique is advantageous because of its simple and continuous processing by online monitoring, helping in commercialization. In certain cases, it is challenging because of the characteristics of drugs or carriers to employ the HME technique for amorphization, and by pretreatment of the blend using any solvent or by employing certain carriers that aid in proper melting and extrusion of the blend, HME can be employed without affecting the nature of the drug [8].

Various techniques can be employed in the preparation of amorphous solid dispersions. HME was preferred over the rest because of its advantages over existing traditional solubility enhancement techniques, which include a continuous mode of

operation; no solvent is needed, even thermolabile compounds can be used as the processing time at higher temperatures is lesser than a minute, disperses the drug in a carrier at the molecular level, etc. The limitations of existing methods include the removal of solvent, separate steps for processing, chances of crystallization because of solvent residues, the inability to apply for thermolabile substances, etc. [9]. The stability of ASDs prepared by amorphous solid dispersion mainly depends on the interaction and bonding between the drug and the carrier [10]. Other parameters like processing parameters, moisture content, and storage conditions also influence the stability of ASDs.

In the present work, quercetin and resveratrol were taken as model compounds that are poorly water-soluble and were studied for enhancement of solubility by amorphous solid dispersion approach employing various carriers like soluplus, kollidon VA 64, PVP K30, kolliphor P407, and P188 at a pre-established ratio of drug: carrier using hot melt extrusion technique. Various studies reported poor solubility of quercetin and resveratrol along with confirmation of its poor bioavailability, which encouraged the development of drug delivery systems for these actives with enhanced solubility and bioavailability.

MATERIALS AND METHODS

Materials

Quercetin and resveratrol were used as model compounds, which were purchased from Herbo Nutra Extracts Pvt. Ltd.; gift samples of polymers like soluplus, PVP K30, kollidon VA64, kolliphor P407, and P188 were obtained from BASF. All the other reagents and chemicals employed were of high-grade purity.

Methods

UV-Visible spectrophotometric method:

Primary stock solutions of 1mg/ml of quercetin in methanol and resveratrol in ethanol were prepared. Later, secondary stock solutions of concentration 100µg/ml were prepared using 1 ml of the initially prepared stock solution and made up to 10 ml with the respective buffer solution (hydrochloric acid buffer pH 1.2, acetate buffer pH 4.5, phosphate buffer pH 6.8, phosphate buffer pH 7.4, or distilled water).

Absorption maxima were observed by scanning the secondary stock solutions from 800 to 200nm, and the spectra were

recorded. Working standards of 2, 4, 6, 8, and 10µg/ml concentrations of quercetin and 1, 2, 3, 4, and 5µg/ml concentrations of resveratrol were prepared by taking 0.2, 0.4, 0.6, 0.8, and 1ml of quercetin secondary stock solution and 0.1, 0.2, 0.3, 0.4 and 0.5 ml of resveratrol secondary stock solution respectively. The volume was made up to 10ml using various buffers and distilled water. Solutions were prepared, absorbances were recorded at respective absorption maxima, and quercetin and resveratrol were calibrated.

Solubility study

Solubility studies of pure quercetin, resveratrol, and fabricated amorphous solid dispersions were carried out by equilibrium solubility studies as per WHO Technical Report series 1019. The highest therapeutic dose of the drug must be dissolved or mixed with 250 ml of the respective solvent or buffer system in less than or equal to 250 ml of the buffer. The highest therapeutic dose of quercetin and resveratrol is 1000mg. An equivalent dose was maintained by adding 100mg of pure quercetin and pure resveratrol to 25 ml of buffer separately (in triplicate).

The solubility studies were carried out by constantly stirring the solution for 24 hours using a rotary shaker at room temperature. The resultant solution was filtered through Whatman filter paper, and the filtrate was analyzed using a UV-visible spectrophotometer against buffer as blank at respective absorption maxima (λ_{max}). The procedure was carried out using above mentioned buffers and distilled water. Similarly, a 10mg active equivalent dose of solid dispersions was added into 2.5ml of distilled water (in triplicate), and after 24h shaking, solubility was analyzed using a spectroscopic method developed earlier.

Preparation of Amorphous solid dispersions [11]

Solid dispersions were fabricated by hot melt extrusion technique using OMICRON 10 PHARMA (Steer Engineering, Bangalore, India) co-rotating twin screw extruder with a diameter of 1.71mm. Bioactive (quercetin, resveratrol) and carrier in different ratios (as given in Table 1) were mixed gently in a glass mortar and pestle, and physical mixtures were made.

Physical mixtures were fed manually into the hopper of the extruder, where barrel temperature was set at 80°C [12] for quercetin mixtures, 110°C [13] for resveratrol physical mixtures, and extruded with a screw speed of 75rpm. The products obtained were stored at room temperature.

Table 1: Formulation table for solid dispersions by hot melt extrusion

SNo	Code	Composition
01	QS-HSD	Quercetin: Soluplus (1:3)
02	QKv-HSD	Quercetin: Kollidon VA 64 (1:3)
03	QKr ₄₀₇ -HSD	Quercetin: Kolliphor P407G (1:5)
04	RS-HSD	Resveratrol: Soluplus (1:5)
05	RKr ₄₀₇ -HSD	Resveratrol: Kolliphor P407G (1:3)
06	RKr ₁₈₈ -HSD	Resveratrol: Kolliphor P188G (1:5)
07	RP-HSD	Resveratrol: PVP K30 (1:5)

H is for Hot melt extrusion, SD is for Solid dispersion, Q is Quercetin, R is Resveratrol, S is Soluplus, Kv is Kollidon VA64, Kr₄₀₇ is Kolliphor P407G, Kr₁₈₈ is Kolliphor P188G, P is PVP K30

Preparation of physical mixtures [14]

The physical mixtures of quercetin and resveratrol with different carriers in the same ratio as formulation composition were prepared to evaluate various parameters and compare with hot melt extruded ASDs. Accurately weighed amounts of drug and carrier were taken into a mortar, triturated thoroughly, passed through 60#, and kept for further analysis.

Fourier transform infrared spectroscopic studies (FTIR) [14,15]

FTIR spectra of quercetin, resveratrol, polymers, their physical mixtures, and solid dispersions were obtained using an attenuated total reflectance (ATR) module of infrared spectrophotometer (ATR-FTIR, Shimadzu, IRSpirit). The spectra were then recorded in the 4000 cm⁻¹ to 650 cm⁻¹ range.

Differential scanning calorimetry (DSC) studies

DSC studies used a differential scanning calorimeter (DSC 60 plus, Shimadzu). All the samples were weighed, and 3-5mg of each sample was taken and analyzed at 10°C/ min using an empty pan as a reference. Pure quercetin, physical mixtures of quercetin with carriers and their respective solid dispersions, were analyzed in the range of 50°C to 350°C [16], and resveratrol, physical mixtures of resveratrol with carriers and solid dispersions from 30°C to 300°C or 450°C [15,17]. Soluplus, kollidon VA64 and kolliphor P188G up to 300°C [18,19], PVP K30 upto 200°C [20] and kolliphor P407G up to 350°C [21].

Particle size [22]

The mean particle size and polydispersity index (PDI) of pure bioactive compounds, carriers, their physical mixtures, and

amorphous solid dispersions were measured using dynamic light scattering (DLS) method using a particle size analyzer (LABINDIA Nano Plus).

Field Emission Scanning electron microscopy (FESEM) studies [18]

The surface morphology of quercetin, resveratrol, carriers, physical mixtures and amorphous solid dispersions was examined using a scanning electron microscope (FEI, QUANTA FEG 250). Samples were made conductive before analysis by sputter coating with gold-palladium alloy, observed at 10 kV accelerated voltage, and the images were taken.

Powder X-ray diffraction (XRD) analysis [14,23,24]

Powder XRD analysis of pure actives, carriers, physical mixtures, and amorphous solid dispersions was carried out to know about the crystallinity of the samples. XRD analysis was performed using a BRUKER D8 Advance diffractometer at an angle from 2° to 50° using Cu radiation with a wavelength 1.54 Å at 40 kV and 40 mA voltage and current, respectively, with a

speed of 2°/min, step size of 0.02° and counting time of 0.5 sec/step.

Statistical analysis [14]

Data was expressed as Mean ± S.D. for three different experiments. $p < 0.05$ was considered statistically significant.

RESULTS AND DISCUSSION

UV-Visible spectrophotometric method

The absorption maxima of quercetin were 254 nm in pH 1.2 and pH 4.5 buffers, 255 nm in phosphate buffers pH 6.8 and pH 7.4, and 256 nm in distilled water. The absorption maxima of resveratrol were 312 nm in pH 1.2, 4.5, and 7.4 buffers, 306 nm in phosphate buffer pH 6.8, and 304 nm in distilled water.

Standard calibration was performed for quercetin and resveratrol in all the mentioned buffers and distilled water. They were found to be linear in Beer's range of 2-10 µg/ml for quercetin, with equations shown in Table 2, and 1-5 µg/ml for resveratrol, with equations shown in Table 3, respectively.

Table 2: Calibration of quercetin in different buffers and distilled water

Buffer	pH 1.2	pH 4.5	pH 6.8	pH 7.4	Distilled water
Conc (µg/ml)	Absorbance (at 254 nm)	Absorbance (at 254 nm)	Absorbance (at 255 nm)	Absorbance (at 255 nm)	Absorbance (at 256 nm)
2	0.069 ± 0.001	0.0506 ± 0.014	0.0597 ± 0.023	0.0646 ± 0.016	0.0933 ± 0.003
4	0.1337 ± 0.027	0.1193 ± 0.009	0.1288 ± 0.017	0.1238 ± 0.011	0.1764 ± 0.026
6	0.1973 ± 0.019	0.1779 ± 0.021	0.1829 ± 0.006	0.1849 ± 0.009	0.2573 ± 0.018
8	0.262 ± 0.011	0.2559 ± 0.011	0.2251 ± 0.012	0.243 ± 0.015	0.3203 ± 0.016
10	0.3333 ± 0.020	0.2999 ± 0.026	0.3178 ± 0.021	0.3147 ± 0.019	0.3854 ± 0.004
equation	$y = 0.033x + 0.0009$	$y = 0.0311x - 0.0047$	$y = 0.0306x - 0.0004$	$y = 0.031x + 0.0002$	$y = 0.0384x + 0.0134$

Table 3: Calibration of resveratrol in different buffers and distilled water

Buffer	pH 1.2	pH 4.5	pH 6.8	pH 7.4	Distilled water
Conc (µg/ml)	Absorbance (at 312 nm)	Absorbance (at 312 nm)	Absorbance (at 306 nm)	Absorbance (at 312 nm)	Absorbance (at 304 nm)
1	0.1262 ± 0.001	0.1550 ± 0.015	0.1461 ± 0.019	0.1325 ± 0.011	0.0945 ± 0.016
2	0.2661 ± 0.012	0.2755 ± 0.011	0.2632 ± 0.008	0.2559 ± 0.024	0.2162 ± 0.022
3	0.4155 ± 0.010	0.4074 ± 0.021	0.3859 ± 0.021	0.3998 ± 0.021	0.3376 ± 0.014
4	0.5328 ± 0.021	0.5122 ± 0.010	0.5095 ± 0.017	0.5187 ± 0.010	0.4710 ± 0.019
5	0.6664 ± 0.003	0.6920 ± 0.013	0.6585 ± 0.020	0.6591 ± 0.017	0.5958 ± 0.011
equation	$y = 0.1343x - 0.0013$	$y = 0.1332x + 0.0072$	$y = 0.1287x + 0.0054$	$y = 0.1314x - 0.0008$	$y = 0.1209x - 0.0163$

Table 4: Solubility of quercetin and resveratrol in different buffers and distilled water

S. No	Sample	Solubility ($\mu\text{g}/\text{ml}$)
01	Quercetin in hydrochloric acid buffer pH 1.2	10.2828 \pm 0.9872
02	Quercetin in acetate buffer pH 4.5	10.8789 \pm 0.7113
03	Quercetin in phosphate buffer pH 6.8	16.9499 \pm 0.4591
04	Quercetin in phosphate buffer pH 7.4	16.7527 \pm 0.7930
05	Quercetin in distilled water	22.9688 \pm 2.7326
06	Resveratrol in hydrochloric acid buffer pH 1.2	28.5431 \pm 2.3361
07	Resveratrol in acetate buffer pH 4.5	17.0420 \pm 3.7605
08	Resveratrol in phosphate buffer pH 6.8	29.3447 \pm 7.4727
09	Resveratrol in phosphate buffer pH 7.4	28.6149 \pm 8.4940
10	Resveratrol in distilled water	52.6606 \pm 4.0960

Table 5: Solubilities of solid dispersions

S. No	Formulation Code	Composition	Solubility (mg/ml)
01	QS-HSD	Quercetin: Soluplus (1:3)	0.823 \pm 0.077
02	QKv-HSD	Quercetin: Kollidon VA 64 (1:3)	0.338 \pm 0.033
03	QKr ₄₀₇ -HSD	Quercetin: Kolliphor P407G (1:5)	0.664 \pm 0.087
04	RS-HSD	Resveratrol: Soluplus (1:5)	5.125 \pm 0.126
05	RKr ₄₀₇ -HSD	Resveratrol: Kolliphor P407G (1:3)	2.412 \pm 0.144
06	RKr ₁₈₈ -HSD	Resveratrol: Kolliphor P188G (1:5)	2.056 \pm 0.195
07	RP-HSD	Resveratrol: PVP K30 (1:5)	0.722 \pm 0.043

Solubility Studies:

Table 4 shows the solubilities of quercetin and resveratrol in various buffers and distilled water. Both bioactives were more soluble in distilled water, with solubilities of 0.023 mg/ml and 0.053 mg/ml for quercetin and resveratrol, respectively. As the solubility of bioactives is high in distilled water, further solubility studies were carried out in distilled water.

Fabrication of ASDs

Solid dispersions were fabricated using the hot melt extrusion (HME) technique with soluplus, kollidon VA 64 as carriers using quercetin in a 1:3 ratio, and with kolliphor P407G in a 1:5 ratio, resveratrol in 1:5 ratios with soluplus, kolliphor P188G, PVP K30 and in 1:3 ratio with kolliphor P407G.

Resveratrol solid dispersions with 1:5 kolliphor P188G and 1:3 kolliphor P407G ratios were prepared and not proceeded further as the product obtained was studied only for solubility and are not feasible for further studies as they are physically unstable (because of their semisolid consistency). All the other solid dispersions were analyzed for solubility and stored at room temperature for further analysis.

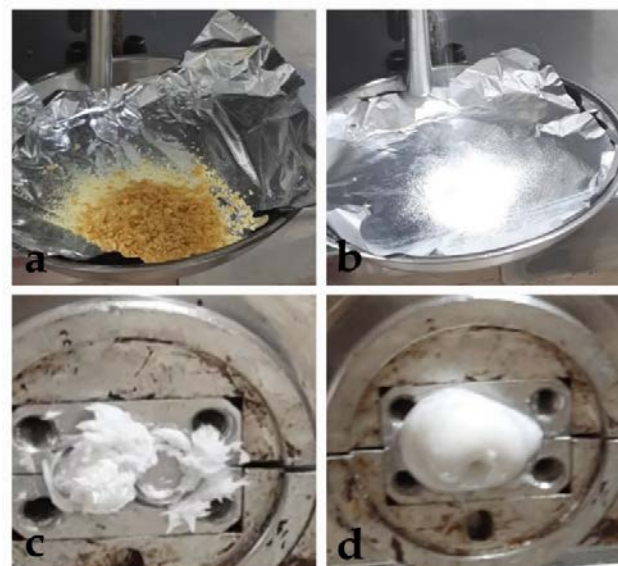


Figure 1: ASDs by HME – a,b represents proper ASDs of quercetin and resveratrol with carriers, and c,d represents ASDs of resveratrol with kolliphors that are semisolids

Solubility studies of ASDs

Equilibrium solubility studies of solid dispersions of quercetin and resveratrol using various carriers in different ratios were

carried out according to WHO protocol in distilled water. The samples were analyzed at 256 nm and 304 nm, respectively. The results are given in Table 5. Quercetin with soluplus exhibited 36 times higher solubility in solid dispersion, and resveratrol solubility was enhanced 97 times with Soluplus by using the hot melt extrusion technique. Of all the carriers employed in the study, soluplus enhanced the solubility of bioactives to a higher extent comparatively.

Fourier Transform InfraRed spectroscopic studies

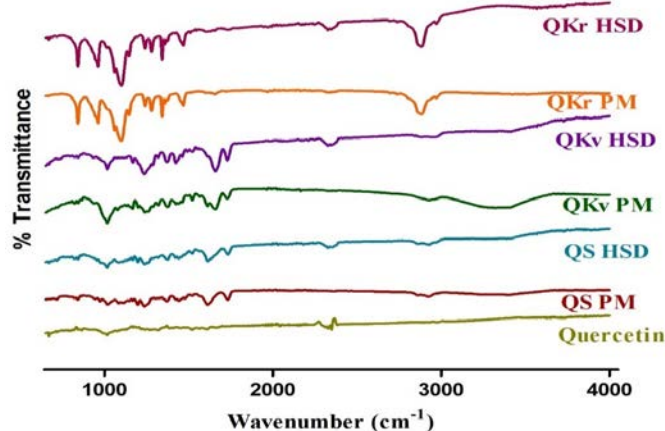


Figure 2: FTIR spectra of pure quercetin (Q), physical mixtures (PM) and HME solid dispersions (HSD) with soluplus (S), kollidon VA64 (Kv) and kolliphor P407G (Kr)

FTIR spectrum of quercetin solid dispersions showed peaks at 1100-1200 cm^{-1} of C-O stretching, broadening peak of polyhydroxy stretching at 3300-3500 cm^{-1} , C=O absorption peak between 1600-1700 cm^{-1} , 1400-1650 cm^{-1} corresponding to C-C stretching and benzene rings, peaks at 1400-1450 cm^{-1} , 850-950 cm^{-1} indicates C-H bending and at 1250-1300 cm^{-1} for C-O stretching of 'O' present in the ring [25,26]. All the characteristic peaks of pure quercetin extract were found in solid dispersions.

The FTIR spectrum of resveratrol showed peaks at 3250-3400 cm^{-1} (polyhydroxy stretching vibrations), 1450-1600 cm^{-1} (stretching vibrations because of the benzene ring), 1600-50 cm^{-1} (aromatic double bonds), and 825-1050 cm^{-1} (bending vibration of C=C-H, i.e., transolefinic bands [27]).

Peaks of resveratrol pure extract were observed in solid dispersions. The peaks of amorphous solid dispersions that correspond to polyhydroxy groups slightly broaden, which might be due to the possible interaction of the active with the carrier.

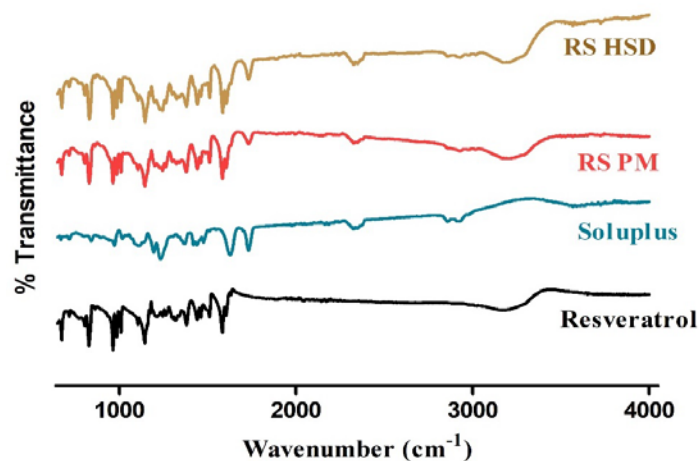


Figure 3: FTIR spectra of pure resveratrol (R), soluplus (S), their physical mixture (PM) & HME solid dispersion (HSD)

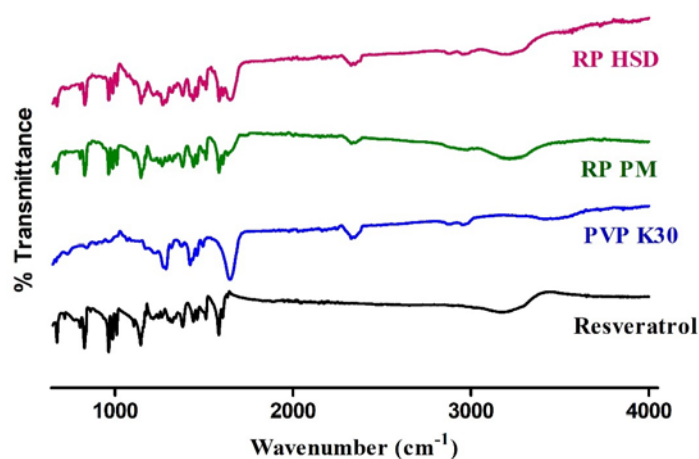


Figure 4: FTIR spectra of pure resveratrol (R), PVP K30 (P), their physical mixture (PM) & HME solid dispersion (HSD)

DSC studies

DSC thermograms of bioactives, selected polymers, their physical mixtures with bioactives, and hot melt extruded solid dispersions were carried out. DSC thermogram of pure quercetin revealed two endothermic peaks corresponding to dehydration at 127.26°C followed by sharp decomposition at 312.71°C [16]. Soluplus exhibited a broad endothermic peak at 60.64°C. Kollidon VA64 revealed an endothermic peak at 56.43°C, and a sharp endothermic peak of kolliphor P407G appeared at 56.37°C. Quercetin: soluplus physical mixture and solid dispersion exhibited a peak around 62°C which corresponds to glass-transition temperature of soluplus, and the sharp peak of decomposition at 312.71°C was not observed in the physical mixture, and a broad peak around 300°C representing decomposition might indicate partial amorphization which

indicates that the drug has been changing to amorphous [16,28]. DSC thermograms of quercetin-kollidon VA64 physical mixture and solid dispersion showed a broad endothermic peak at 58°C-63°C which is the characteristic peak of kollidon VA64, a sharp peak around 131°C in the physical mixture of a result of glass-transition temperature, dehydration of quercetin and absence of sharp decomposition peak at 312°C in the physical mixture and solid dispersion reveals that the drug is being amorphized [16,20]. Thermograms of quercetin-kolliphor P407G physical mixture and solid dispersion had a sharp endothermic peak at 52°C-56°C indicating glass-transition temperature as well as the specific peak of kolliphor P407G, an endothermic peak around 314°C followed by an exothermic peak in physical mixture might represent the crystalline nature of quercetin and absence of an endothermic peak at 312°C in solid dispersion after the exothermic peak indicates that the nature of quercetin has been changing to amorphous [16,21]. DSC thermogram of pure

resveratrol showed exothermic peak at 267.67°C [15]. Kolliphor P188G was characterized by a sharp endothermic peak at 54.63°C, and PVP K30 showed a broad endothermic peak at 78.93°C. Resveratrol: soluplus physical mixture revealed two peaks of which a broad endothermic peak at 61.75°C represents the glass-transition temperature of soluplus and broad endothermic peak at 280.23°C is of resveratrol. The peak at 59°C in the thermogram of solid dispersion is the glass-transition temperature of the soluplus, and the absence of a resveratrol characteristic peak at 267.1°C states the amorphization of the drug [15,28]. Thermograms of resveratrol-PVP K30 physical mixture and solid dispersion had a broad endothermic peak at 65°C-79°C that characterizes PVP K30, a sharp glass-transition peak around 150°C in physical mixture and absence of sharp decomposition peak at 267°C in both physical mixture and solid dispersion revealed that crystalline form of resveratrol was converted to amorphous [15,20].

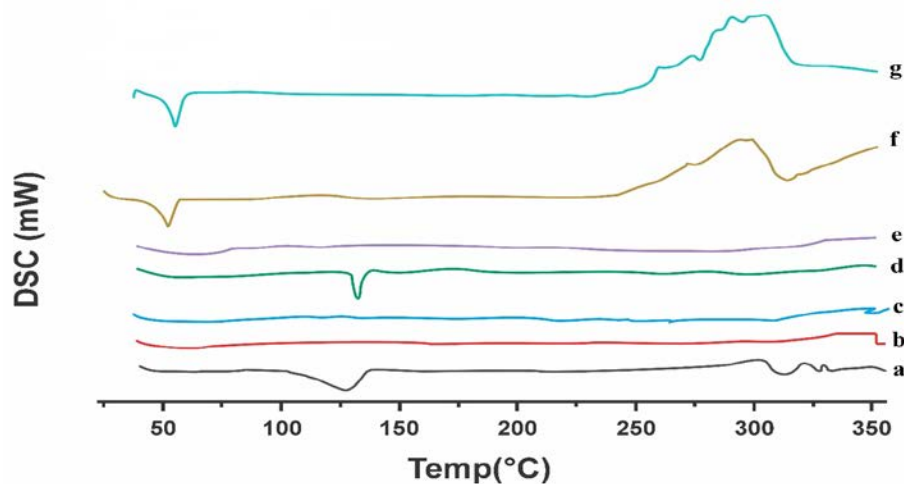


Figure 5: DSC thermograms of a. Quercetin (Q), b. QS PM, c. QS HSD, d. QKv PM, e. QKv HSD, f. QKr PM and g. QKr HSD where PM - physical mixture, HSD - HME solid dispersion, S – soluplus, Kv - kollidon VA64 and Kr - kolliphor P407G.

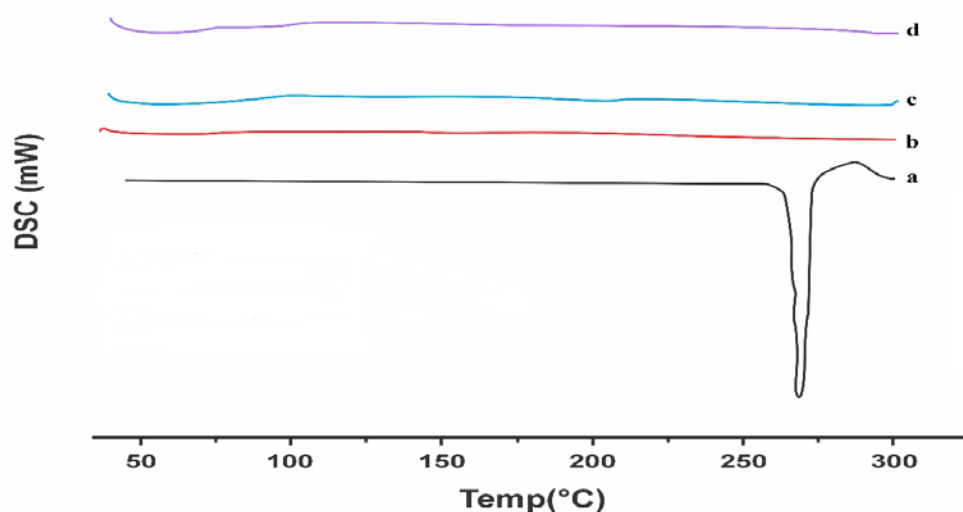


Figure 6: DSC thermograms of a. Resveratrol (R), b. Soluplus (S), c. RS physical mixture and d. RS HME solid dispersion.

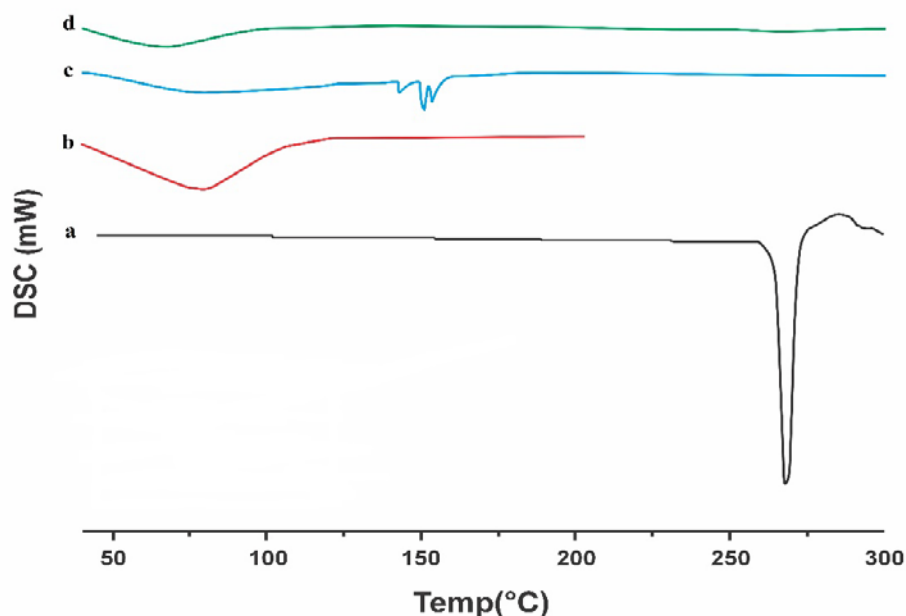


Figure 7. DSC thermograms of a. Resveratrol (R), b. PVP K30 (P), c. RP physical mixture and d. RP HME solid dispersion

Particle Size

Particle size analysis using the DLS method was carried out for pure quercetin and resveratrol extracts, polymers, their physical mixtures and fabricated amorphous solid dispersions were reported in Table 6. The mean particle size of quercetin was $1.53 \pm 0.08 \mu\text{m}$ with a poly-dispersity index (PDI) of 0.399; the least particle size of quercetin was $0.48 \pm 0.06 \mu\text{m}$ with a 3.2-fold decrease in quercetin and soluplus dispersion with a PDI of 0.314. Similarly, the mean particle size of pure resveratrol was

$10.26 \pm 2.89 \mu\text{m}$ with a PDI of 0.971; the particle size of $0.22 \pm 0.09 \mu\text{m}$ with a PDI of 0.158 was observed with resveratrol and soluplus solid dispersion which was 47 times lower than resveratrol. A reduced polydispersity index value indicates that the mixture contains almost similar-sized particles, i.e., uniform particle size distribution, which interacts alike with the solvent and results in high solubility. If the PDI values are higher, the mixture contains particles of different sizes, which have varied interactions with the solvent, making it less soluble.

Table 6: Particle size analysis by Dynamic light scattering (DLS)

SNo	Sample	Average particle size (μm)	Polydispersity index (PDI)	D10 (μm)	D50 (μm)	D90(μm)
01	Pure quercetin (Q)	1.53 ± 0.08	0.399	0.91 ± 0.01	1.13 ± 0.01	19.11 ± 15.41
02	Pure resveratrol (R)	10.26 ± 2.89	0.971	3.65 ± 1.03	48.79 ± 27.01	124.19 ± 14.12
03	Soluplus	0.06 ± 0.00	0.046	0.05 ± 0.00	0.06 ± 0.00	0.08 ± 0.01
04	Kolliphor P407G	2.04 ± 1.77	1.191	0.01 ± 0.01	19.68 ± 17.49	28.67 ± 17.23
05	Kollidon VA64	0.93 ± 0.10	0.575	0.01 ± 0.00	0.11 ± 0.17	23.68 ± 4.82
06	PVP K30	1.77 ± 0.20	1.074	0.01 ± 0.01	17.92 ± 15.08	42.65 ± 16.22
07	QS PM	0.95 ± 0.26	0.593	0.03 ± 0.00	7.39 ± 12.73	23.53 ± 9.04
08	QS HSD	0.48 ± 0.06	0.314	0.04 ± 0.00	0.05 ± 0.00	8.43 ± 1.67
09	QKr PM	3.17 ± 0.96	1.353	0.55 ± 0.10	29.42 ± 4.35	44.78 ± 12.81
10	QKr HSD	2.57 ± 0.17	1.305	0.27 ± 0.01	24.68 ± 2.02	34.13 ± 2.32
11	QKv PM	4.60 ± 0.41	1.929	0.58 ± 0.03	27.99 ± 5.87	37.73 ± 8.02
12	QKv HSD	1.60 ± 0.15	0.773	0.46 ± 0.01	18.47 ± 4.84	31.76 ± 2.25
13	RS PM	0.37 ± 0.15	0.245	0.04 ± 0.00	0.04 ± 0.00	4.55 ± 4.53
14	RS HSD	0.22 ± 0.09	0.158	0.05 ± 0.00	0.09 ± 0.01	1.62 ± 2.44
15	RP PM	6.13 ± 1.57	2.891	6.78 ± 11.16	26.74 ± 0.57	35.02 ± 0.67
16	RP HSD	3.19 ± 1.33	1.802	0.03 ± 0.01	31.67 ± 4.11	43.12 ± 7.45

FESEM studies

Scanning electron microscopic studies of pure quercetin, resveratrol, polymers, their physical mixtures, and various solid dispersions were carried out, and the micrographs were shown in Figure 8. It was observed that pure quercetin, pure resveratrol, QS PM, and RS PM depicted well-defined crystal structures of the bioactive; in soluplus, QS HSD, and QKr HSD, the particles were not seen indicating glassy solution-like texture; in kolliphor P407G crystal structure disappeared and exhibited complete spherical, smooth surface morphology; PVP K30, RS HSD, and kollidon VA64 showed smooth irregular surface and in QKr PM, QKv PM, QKv HSD, RP PM and RP HSD, the crystal structures which are of bioactive appeared on the surface that are embedded into the respective carriers and is with rough and irregular shape [29].

Considering the Noyes-Whitney dissolution model, the drug's surface area is directly proportional to its dissolution rate. Similarly, reduced particle size has higher solubility due to the availability of a larger surface area that can interact with the solvent. Spherical particles have a higher surface area than irregular particles, which have a better area than crystalline forms. In this case, spherical and irregular particles with reduced particle size resulted in higher solubility, which, in turn, helps in the drug's better dissolution and bioavailability.

Powder XRD analysis [7,24,35]

Powder XRD analysis was used to study the crystallinity and nature of bioactives in their pure forms, physical mixtures, and fabricated solid dispersions. Pure quercetin is characterized by sharp peaks at 10.86°, 12.53°, and 27.47°, indicating its crystalline nature. Resveratrol pure extract exhibited a crystalline nature depicted by characteristic peaks at 6.67°, 13.31°, 16.44°, 22.43°, 23.48°, 25.32° and 28.38°. Polymers like soluplus, kollidon VA64, and PVP K30 were amorphous, and kolliphor P407G exhibited two characteristic peaks at 19.27° and 23.41°.

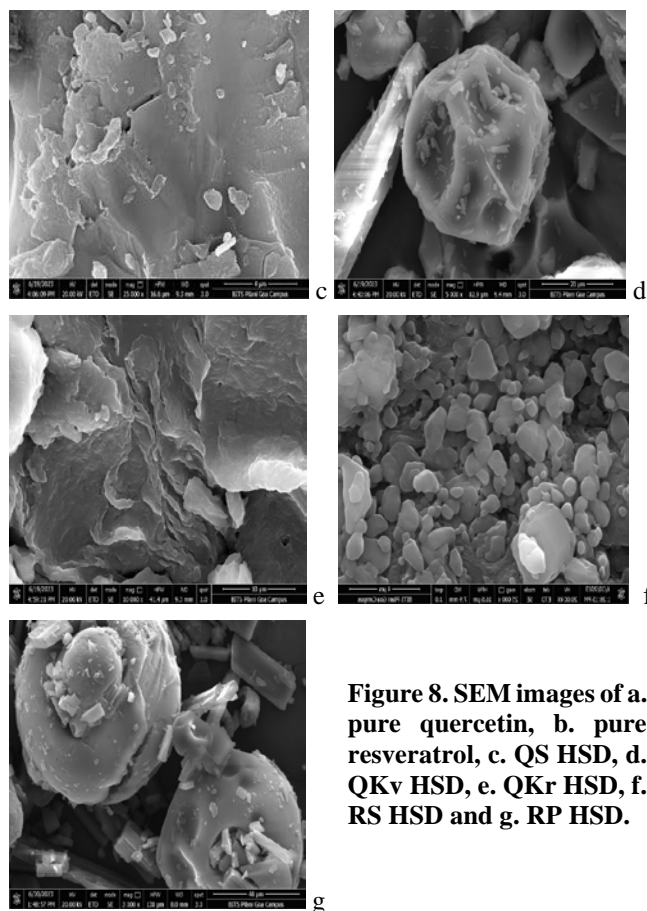
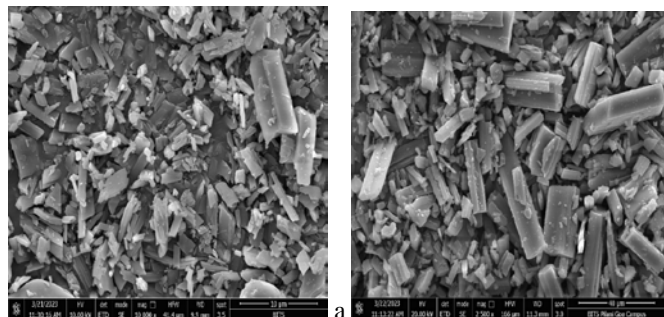


Figure 8. SEM images of a. pure quercetin, b. pure resveratrol, c. QS HSD, d. QKv HSD, e. QKr HSD, f. RS HSD and g. RP HSD.

Using Soluplus as carrier, the three prominent characteristic peaks of quercetin were observed in the physical mixture. Still, only one peak was seen in solid dispersion with reduced intensity, which may result in partial amorphization. In the case of kollidon VA64, the three main characteristic peaks of quercetin were observed in the physical mixture and solid dispersion but with reduced intensities, which might be due to the dilution effect of the carrier. When kolliphor P407G was employed as a carrier, the two prominent characteristic peaks of polymer were observed in the physical mixture and solid dispersion prepared with reduced intensities. The characteristic sharp peaks of quercetin were not observed, indicating the amorphization of the drug as shown in Figure 9. All the characteristic peaks of pure resveratrol were observed with minimal intensities in a physical mixture with soluplus and few peaks with reduced intensities in solid dispersion by HME, indicating conversion of crystalline form to amorphous form (Figure 10). All the characteristic peaks of pure resveratrol were observed with minimal intensities in a physical mixture with PVP K30 and few peaks with reduced intensities in solid dispersion by HME, indicating conversion of crystalline form to amorphous form (Figure 11).

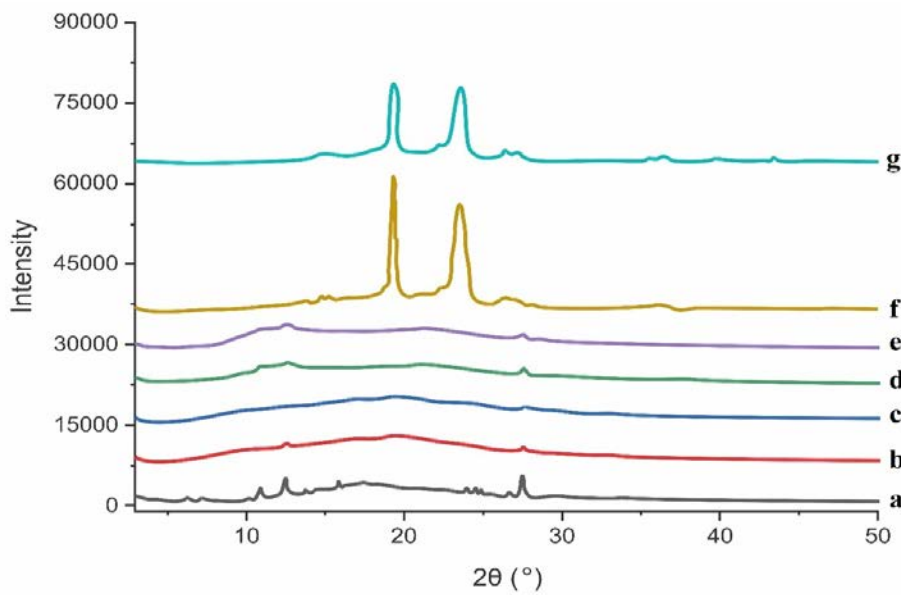


Figure 9: X-ray diffractograms of a. Quercetin (Q), b. QS PM, c. QS HSD, d. QKv PM, e. QKv HSD, f. QKr PM and g. QKr HSD where PM - physical mixture, HSD - HME solid dispersion, S – soluplus, Kv - kollidon VA64 and Kr - kolliphor P407G

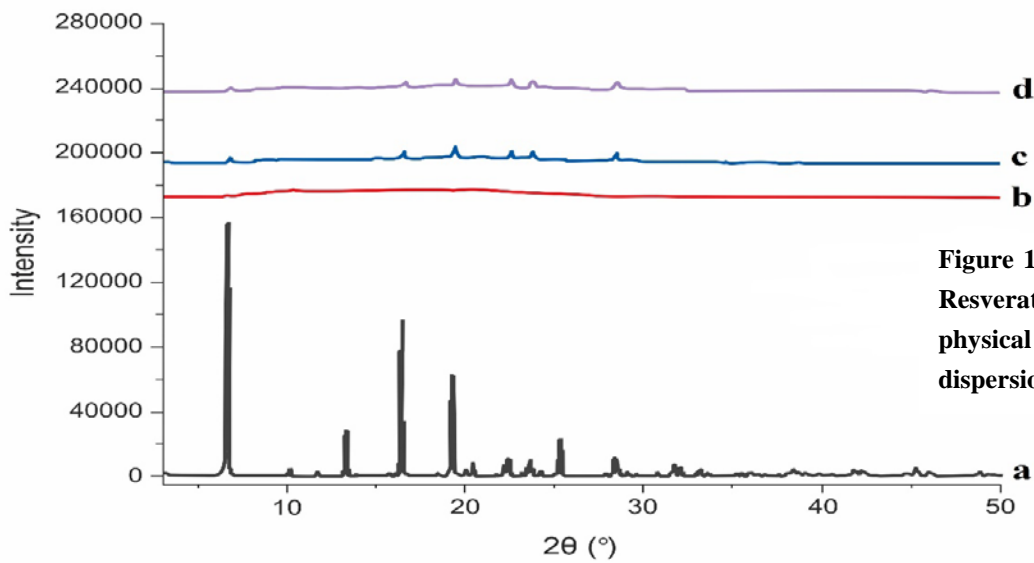


Figure 10: X-ray diffractograms of a. Resveratrol (R), b. Soluplus (S), c. RS physical mixture and d. RS HME solid dispersion

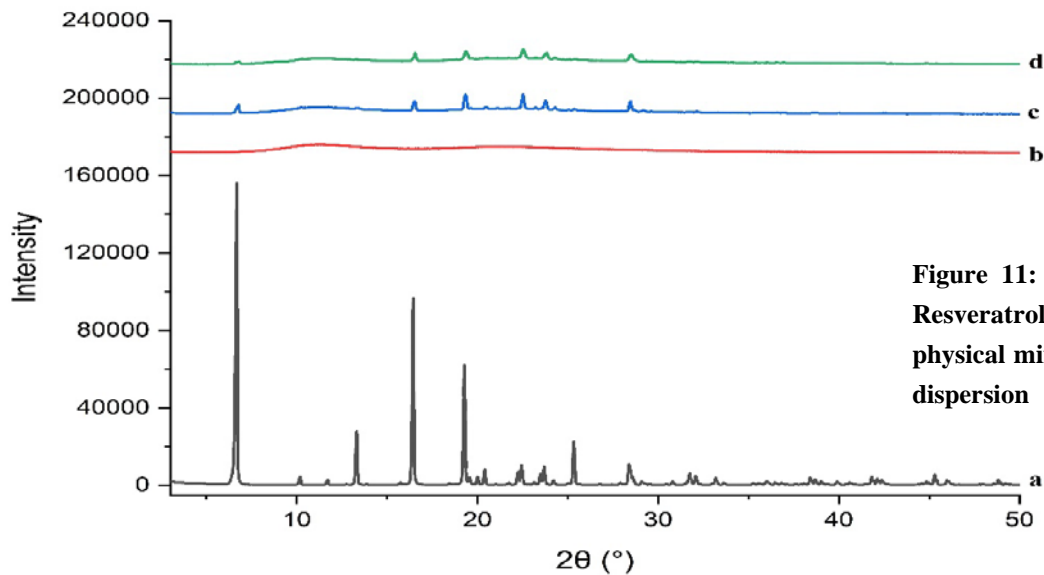


Figure 11: X-ray diffractograms of a. Resveratrol (R), b. PVP K30 (P), c. RP physical mixture, and d. RP HME solid dispersion

This work focused on studying the hot melt extrusion technique to increase solubility. Table 7 gives an overall summary of the work that compares the bioactive compound before and after

HME. Soluplus was prioritized and mentioned, considering all the studies.

Table 7: Comparison of properties of quercetin and resveratrol before and after HME

Parameter	Quercetin	Quercetin- soluplus HME SD	Resveratrol	Resveratrol- soluplus HME SD
Solubility (mg/ml)	0.023	0.823	0.053	5.125
Particle size (µm)	1.53	0.48	10.26	0.22
Polydispersity index	0.399	0.314	0.971	0.158

CONCLUSION

Among many techniques for producing amorphous solid dispersions, this work explored the hot melt extrusion technique using quercetin and resveratrol as model drugs employing various carriers. ASDs of bioactives with pre-established drug-to-carrier ratios were fabricated and characterized using different methods like DSC, PXRD, etc., and solubility assessment. The results demonstrated that hot melt extrusion significantly improved the solubility of both quercetin and resveratrol and crystalline forms were transformed into amorphous forms, as confirmed by DSC thermograms and XRD diffractograms.

There was a reduction in particle size and polydispersity index, which contributed to enhanced solubility. This research established HME as a useful approach for fabricating amorphous solid dispersions. Further, this work can be studied for pilot batches and optimization of pilot batches, which helps for commercial scalability. *In vivo* studies can be performed based on the work, as the selected bioactives have various therapeutic and nutraceutical benefits.

ACKNOWLEDGEMENTS

Authors are thankful to Mr. Kumar Kanneboina and Ms. Yarram Jyothi from CSIF, BITS Pilani KK Birla Goa Campus for smooth conduct of analysis and characterizations. Authors feel grateful towards BASF and Herbo Nutra Pvt. Ltd. for timely issue of gift sample of soluplus and purchase of resveratrol extract respectively. Authors are also thankful to The Principal, Staff and Management of KLE College of Pharmacy, Hubli; constituent units of KAHER and The Principal, Staff and Management of Manipal College of Pharmaceutical Sciences, Manipal and Steer Life Sciences Pvt. Ltd. (Bangalore) for providing the facilities needed to carry out this work.

FINANCIAL ASSISTANCE

NIL

CONFLICT OF INTEREST

The authors declare no conflict of interest.

AUTHOR CONTRIBUTION

Lakshmi Swapna Sai contributed to the idea of the work, carried out the studies in the laboratory, collected, analyzed, and interpreted the data, and drafted and revised the manuscript. Fatima S Dasankoppa contributed to the idea of the work, guided the studies, and drafted and revised the manuscript critically. Srinivas Mutalik guided the studies and revised the manuscript. Muralidhar Pisay carried out a part of the work, analyzed the data, and revised the manuscript. All the authors read, revised and approved the submitted version of the manuscript.

REFERENCES

- [1] Anna K, Kyriakos K, Ioannis N. Co-amorphous solid dispersions for solubility and absorption improvement of drugs: Composition, preparation, characterization and formulations for oral delivery. *Pharmaceutics*, **10**(3), 98 (2018) <https://doi.org/10.3390/pharmaceutics10030098>
- [2] Andre H, Johanna M, Hanlin L, Christian J, Andrea M, Bart H et.al. Challenges and strategies for solubility measurements and dissolution method development for amorphous solid dispersion formulations. *AAPS J.*, **25**(1), 11 (2022) <https://doi.org/10.1208/s12248-022-00760-8>
- [3] Thomas WYL, Nathan AB, Hui HW, Chow SF, Wan KY, Albert HLC. Delivery of poorly soluble compounds by amorphous solid dispersions. *Curr Pharm Des.*, **20**(3), 303-24 (2014) <http://dx.doi.org/10.2174/13816128113199990396>
- [4] Hou HH, Aniruddha R, Keyur MP, Joseph WL, Ariel M, Edward Y, Wei J, Karthik N. Impact of method of preparation of amorphous solid dispersions on mechanical properties: comparison of coprecipitation and spray drying. *J Pharm Sci.*, **108**(2), 870-9 (2019) <https://doi.org/10.1016/j.xphs.2018.09.008>
- [5] Kramarczyk D, Knapik-Kowalczyk J, Kurek M, Jamróz W, Jachowicz R, Paluch M. Hot Melt Extruded Posaconazole-Based Amorphous Solid Dispersions—The Effect of Different Types of

- Polymers. *Pharmaceutics*, **15**(3), 799 (2023)
<https://doi.org/10.3390/pharmaceutics15030799>
- [6] Xiangyu M, Robert OW. Characterization of amorphous solid dispersions: An update. *J Drug Deliv Sci Technol.*, **50**, 113-24 (2019) <https://doi.org/10.1016/j.jddst.2019.01.017>
- [7] Wenling F, Wenjing Z, Xinyi Z, Yan X, Liuqing D. Application of the combination of ball-milling and hot-melt extrusion in the development of an amorphous solid dispersion of a poorly water-soluble drug with high melting point. *RSC Adv.*, **9**, 22263-73 (2019) <https://doi.org/10.1039/C9RA00810A>
- [8] Wenjing Z, Wenling F, Xiaotong Z, Meiqi G. Sustained-release solid dispersion of high-melting-point and insoluble resveratrol prepared through hot melt extrusion to improve its solubility and bioavailability. *Molecules*, **26**, 4982 (2021)
<https://doi.org/10.3390/molecules26164982>
- [9] Nicole M, Bjad A, Venkata RK, Sandeep S, Priyanka T, Suresh B, Michael AR. Manufacturing strategies to develop amorphous solid dispersions: An overview. *J Drug Deliv Sci Technol.*, **55**, 101459 (2020) <https://doi.org/10.1016/j.jddst.2019.101459>
- [10] Jiawei H, Mengyuan T, Yang Y, Wen S, Zhimin Y, Yunran Z, Yijun Z, Xiaoqian L, Jue W. Amorphous solid dispersions: Stability mechanism, design strategy and key production of hot melt extrusion. *Int J Pharm.*, **646** (2023)
<https://doi.org/10.1016/j.ijpharm.2023.123490>
- [11] Muralidhar P, Dani LY, Sai KAV, Krishnamurthy B, Koteswara KB, Srinivas M. Effervescence induced amorphous solid dispersions with improved drug solubility and dissolution. *Pharm Dev Technol.*, **28**(2), 176-89 (2023)
<https://doi.org/10.1080/10837450.2023.2172039>
- [12] Chia MK, Wai KN, Parijat K, Kok PC, Yuancai D. Hot-melt extrusion microencapsulation of quercetin for taste-masking. *J Microencapsul.*, **34**(1), 29-37 (2017)
<https://doi.org/10.1080/02652048.2017.1280095>
- [13] Huanyue Z, Yu W, Shuting L, Ming L. Improving chemical stability of resveratrol in hot melt extrusion based on formation of eutectic with nicotinamide. *Int J Pharm.*, **607**, 121042 (2021)
<https://doi.org/10.1016/j.ijpharm.2021.121042>
- [14] Nabil KA, Ameenuzzafar Z, Syed SI, Khalid SA, Sultan A, Tilal E, Fadhel AA, Sultan A, Usama AF, Nabil AA, Mohammed SA. Formulation of amorphous ternary solid dispersions of dapagliflozin using PEG 6000 and Poloxamer188: Solid-state characterization, Ex-vivo study, and molecular simulation assessment. *Drug Dev Ind Pharm.*, **46**(9), 1458-67 (2020)
<https://doi.org/10.1080/03639045.2020.1802482>
- [15] Khalid AA, Pradeep RV, Francesco T, Roberta C. Cyclodextrin-based nanospheres for delivery of resveratrol: *in vitro* characterisation, stability, cytotoxicity and permeation study. *AAPS PharmSciTech.*, **12**(1), 279-86 (2011)
<https://doi.org/10.1208/s12249-011-9584-3>
- [16] Khalid AM, Mohammed AA, Shahid J, Ramadan AS, Mohammad NA, Faiyaz S. Development and evaluation of PLGA polymer-based nanoparticles of quercetin. *Int J Bio Macromol.*, **92**, 213-9 (2016)
<https://doi.org/10.1016/j.jbiomac.2016.07.002>
- [17] Gangqi H, Bing W, Mengli J, Shuxin D, Wenxuan Q, Yuxuan M, Zhimei M, Yuhao Q, Wenxing Z, Xinli L, Wei L. Optimization and evaluation of resveratrol amorphous solid dispersions with a novel polymeric system. *Math Biosci Eng.*, **19**(8), 8019-34 (2022) <https://doi.org/10.3934/mbe.2022375>
- [18] Jaywant NP, Rahul TS, Avinash BG, Kailas KM, Sharadchandra DJ, Divakar RJ, Purnima DA. Development of amorphous dispersions of artemether with hydrophilic polymers via spray drying: Physicochemical and *in silico* studies. *Asian J Pharm Sci.*, **11**(3), 385-95 (2016)
<https://doi.org/10.1016/j.ajps.2015.08.012>
- [19] Meena MK, Choudhary D, Chouhan M, Shukla P, Sinha SK. Enhancement of solubility and dissolution rate of erlotinib hydrochloride by solid dispersion technique with poloxamer 188: preparation and *in-vitro* evaluation. *Int J Pharm Sci Res.*, **11**(1), 387-93 (2020) [https://doi.org/10.13040/ijpsr.0975-8232.11\(1\).387-93](https://doi.org/10.13040/ijpsr.0975-8232.11(1).387-93)
- [20] Siok-Yee C, Yin-Ying C, Xin-Zi C, Eryn YT, Joan Q. The characterization and dissolution performances of spray dried solid dispersion of ketoprofen in hydrophilic carriers. *Asian J Pharm Sci.*, **10**(5), 372-85 (2015)
<https://doi.org/10.1016/j.ajps.2015.04.003>
- [21] Sakal M, Arafat M, Yuvaraju P, Beiram R, Aburuz S. Preparation and characterization of theophylline controlled release matrix system incorporating poloxamer 407, stearyl alcohol, and hydroxypropyl methylcellulose: A novel formulation and development study. *Polymers*, **16**(5), 643 (2024)
<https://doi.org/10.3390/polym16050643>
- [22] Hussain T, Paranthaman S, Rizvi SMD, Moin A, Gowda DV, Subaiea GM, Ansari M, Alanazi AS. Fabrication and Characterization of Paclitaxel and Resveratrol Loaded Soluplus Polymeric Nanoparticles for Improved BBB Penetration for Glioma Management. *Polymers*, **13**(19), 3210 (2021)
<https://doi.org/10.3390/polym13193210>
- [23] Doreth M, Hussein MA, Priemel PA, Grohganz H, Holm R, Diego HL, Rades T, Lobmann K. Amorphization within the tablet: Using microwave irradiation to form a glass solution in situ. *Int J Pharm.*, **519**(1-2), 343-51 (2017)
<http://dx.doi.org/10.1016/j.ijpharm.2017.01.035>
- [24] Sumit K, Brian L, Yin-Chao T. A new combination approach of CI jet and QESD to formulate pH-susceptible amorphous solid dispersions. *Int J Pharm.*, **466**, 368-74 (2014)
<https://doi.org/10.1016/j.ijpharm.2014.03.042>
- [25] Hector P, David Q, Juan DF, Camila MM, Etelvino HBJ, Luis AG, Sandra M. Antioxidant effects of quercetin and catechin

- encapsulated into PLGA nanoparticles. *J Nanomater.*, **2012**, 145380 (2012) <https://doi.org/10.1155/2012/145380>
- [26] Mayur B, Zaved AK. Poly(n-butylcyanoacrylate) nanoparticles for oral delivery of quercetin: preparation, characterization and pharmacokinetics and biodistribution studies in wistar rats. *Int J Nanomedicine*, **10(1)**, 3921-35 (2015) <https://doi.org/10.2147/IJN.S80706>
- [27] Yaning S, Fan Y, Keyu L, Qianru H, Ming M. Characterizations and bioavailability of dendrimer-like glucan nanoparticulate system containing resveratrol. *J Agric Food Chem.*, **68(23)**, 6420-9 (2020) <https://doi.org/10.1021/acs.jafc.0c01315>
- [28] Saad MA, Wenli L, Jun-Bom P, Joseph TM, Bader BA, Soumyajit M, Nigel L, Karl K, Andreas G, Michael AR. Stability-enhanced hot-melt extruded amorphous solid dispersions via combinations of soluplus and HPMCAS-HF. *AAPS PharmSciTech.*, **16**, 824-34 (2015) <https://doi.org/10.1208/s12249-014-0269-6>
- [29] Zafar A, Alruwaili NK, Imam SS, Alsaidan OA, Alkholifi FK, Alharbi KS, Mostafa EM, Alanazi AS, Gilani SJ, Musa A, Alshehri S, Rawaf A, Aliquraini A. Formulation of Genistein-HP _ Cyclodextrin-Poloxamer 188 Ternary Inclusion Complex: Solubility to Cytotoxicity Assessment. *Pharmaceutics*, **13(12)**, 1997 (2021) <https://doi.org/10.3390/pharmaceutics13121997>
- [30] Xianbao S, Na F, Gang Z, Jin S, Zhonggui H, Jing L. Quercetin amorphous solid dispersions prepared by hot melt extrusion with enhanced solubility and intestinal absorption. *Pharm Dev Technol.*, **25(4)**, 472-81 (2021) <https://doi.org/10.1080/10837450.2019.1709502>